Edith Cowan University
Research Online

ECU Publications Pre. 2011

2007

Wavelength-encoded OCDMA system using Opto-VLSI processors

Muhsen Aljada
Edith Cowan University

Kamal Alameh
Edith Cowan University

This article was originally published as: Aljada, M. , & Alameh, K. (2007). Wavelength-encoded OCDMA system using Opto-VLSI processors. Optics Letters, 32(13), 1782-1784. This paper was published in Optics Letters and is made available as an electronic reprint with the permission of OSA. The paper can be found at the following URL on the OSA website: http://www.opticsinfobase.org/abstract.cfm?URI=ol-32-13-1782. Systematic or multiple reproduction or distribution to multiple locations via electronic or other means is prohibited and is subject to penalties under law.
This Journal Article is posted at Research Online.
http://ro.ecu.edu.au/ecuworks/1509

Wavelength-encoded OCDMA system using opto-VLSI processors

Muhsen Aljada and Kamal Alameh*

Centre of Excellence for MicroPhotonic Systems, Electron Science Research Institute, Edith Cowan University, Joondalup WA6027, Australia

**Corresponding author: m.aljada@ecu.edu.au*

Received March 1, 2007; revised March 30, 2007; accepted April 27, 2007; posted May 3, 2007 (Doc. ID 80491); published June 18, 2007

We propose and experimentally demonstrate a 2.5 Gbits/s per user wavelength-encoded optical code-division multiple-access encoder–decoder structure based on opto-VLSI processing. Each encoder and decoder is constructed using a single 1D opto-very-large-scale-integrated (VLSI) processor in conjunction with a fiber Bragg grating (FBG) array of different Bragg wavelengths. The FBG array spectrally and temporally slices the broadband input pulse into several components and the opto-VLSI processor generates codewords using digital phase holograms. System performance is measured in terms of the autocorrelation and cross-correlation functions as well as the eye diagram. © 2007 Optical Society of America

OCIS codes: 070.4550, 060.2330, 060.2630, 090.1970.

Over recent years, optical code-division multiple-access (OCDMA) systems have been investigated for local area networks (LANs), and have received significant attention for their ability to increase the number of active users and provide multiple-user access over the same bandwidth. In OCDMA systems, each user is typically assigned a unique signature (or code), which is spread in time and/or frequency and designed to minimize the interchannel interference and to maximize the spectrum utilization. The key components of OCDMA systems are the encoder and the decoder that perform all-optical code generation and data recognition, respectively [1]. A code or sequence of pulses referred to as "chips" is attributed to each user to encode its data bits. The encoded data are then broadcast into the network and recognized only by the matched decoder.

Various OCDMA implementation techniques have been proposed, including direct-sequence encoding [1], wavelength encoding [2–4], spectral-phase encoding [5], spectral-amplitude coding [6], two-dimensional (2D) encoding [7], and hybrid coding approaches [8]. Most wavelength-encoding OCDMA coding designs have so far been based on using optical filters, such as fiber Bragg gratings (FBGs). However, OCDMA systems based on such designs require N-1 encoders for each user (N is the number of users in the network) as well as an optical switch to select the proper encoder. The use of an optical switch and FBGs that can be tuned in real time makes such OCDMA systems impractical because it limits the flexibility, accuracy, and variety of the encoding–decoding operation.

In this Letter, we propose a wavelength-encoded OCDMA encoder–decoder structure employing an FBG array that spectrally and temporally slices the broadband input pulse into several chips in conjunction with an opto-very-large-scale-integrated (VLSI) processor [9] that generates codewords through digital phase holograms. The proof-of-concept of the proposed OCDMA encoder–decoder structure is demonstrated at 2.5 Gbits/s.

The structure of the proposed OCDMA encoder–decoder is shown by the experimental setup in Fig. 1. The encoder of a transmitter consists of an array of equally spaced FBGs of different Bragg wavelengths. The FBG array spectrally slices an incoming broadband optical pulse into several chips of different wavelengths. These chips are equally spaced by a chip interval corresponding to the round-trip propa-

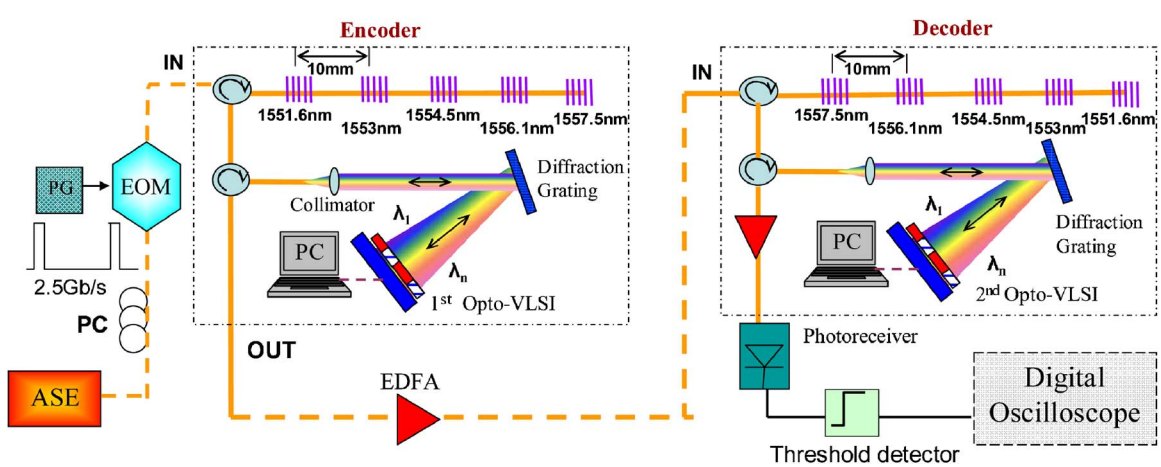

Fig. 1. (Color online) Wavelength-encoded OCDMA encoder–decoder structure.

0146-9592/07/131782-3/$15.00 © 2007 Optical Society of America

gation between two adjacent Bragg gratings. It is important that, to avoid chip collision, all the chips should exit the FBG array before the next pulse is launched. Subsequently, all the chips are routed to a 1 mm diameter collimator and launched to a 1200 line/mm grating plate. The latter spreads the wavelength components of the collimated beam along different directions and maps them onto the active window of the first opto-VLSI processor (encoder). The opto-VLSI processor comprises an array of liquid crystal (LC) cells independently driven electronically by a VLSI circuit that generates multiphase digital holographic diffraction gratings capable of steering and/or shaping optical beams. The steering capability of opto-VLSI processors was previously reported in [9].

Each wavelength component incident onto the opto-VLSI processor is assigned a pixel block loaded with an optimized digital phase hologram so that the optical power falling on that pixel block is independently either reflected back along its incident optical path, and hence coupled into the fiber collimator with minimum attenuation, or appropriately steered off track, so its power is not coupled back into the fiber collimator; thus a codeword can be generated. The wavelength components coupled into the fiber through the collimation lens are routed through an optical circulator and amplified using an erbium-doped fiber amplifier (EDFA). The encoded signal is then transmitted into the network.

At the receiver side, the encoded signal is routed to an FBG array similar to that of the transmitter but arranged in a reversed order. The receiver's FBG array realigns all chips into a single-pulse time slot. Subsequently, the signal is routed to a fiber collimator and the collimated optical beam is launched toward a diffraction grating plate, which spreads the wavelength components along different directions and maps them onto the active window of the decoding opto-VLSI processor. It is important to note that to retrieve the original signal, the second opto-VLSI processor must be loaded with digital phase holograms similar to those of the first opto-VLSI processor. The decoded signal is coupled back into the fiber collimator and routed through an optical circulator to an EDFA that amplifies the optical signal before detection by the photoreceiver. When the digital-phase holograms of the encoder and decoder are matched, a high-peak autocorrelation waveform is generated, which can be recognized using a threshold detector. Otherwise, a low-amplitude cross-correlation function is generated, indicating a mismatch between the codewords of the encoder and the decoder.

To prove the principle of the proposed structure, a low-coherent amplified spontaneous emission (ASE) source was launched into an electro-optic modulator (EOM) and intensity-modulated with a non-return-to-zero periodic pattern "10,000" at 12.5 Gbits/s (this is equivalent to a 2.5 Gbits/s return-to-zero pattern with a 20% duty cycle). The modulated light was launched into an optical fiber having an array of five fiber FBGs equally spaced, with center-to-center spacing of 10 mm. All FBGs had identical reflectivities of 90% and Bragg wavelengths of $\lambda_1 = 1551.6$ nm, $\lambda_2 = 1553$ nm, $\lambda_3 = 1554.5$ nm, $\lambda_4 = 1556.1$ nm, and $\lambda_5 = 1557.5$ nm, respectively.

Both 1D opto-VLSI processors used in the experiments had 1×4096 pixels and 256 phase levels, with 1 μm pixel size, and 0.8 μm spacing. They were controlled by using LABVIEW software to generate optimized digital holograms that selectively steer the incident wavelength components along arbitrary directions. The 256 voltage levels applied to the individual pixels were between 0 and 2 V.

The first opto-VLSI processor was configured to generate a codeword employing λ_1, λ_2, and λ_3. Therefore, the wavelengths λ_1, λ_2, and λ_3 were coupled back into the collimator, while the wavelengths λ_4 and λ_5 were substantially attenuated (steered away). Figure 2(a) shows the schematic of the phase holograms loaded on the first opto-VLSI processor. Figure 2(b) shows the measured spectrum of the optical signal coupled back into the collimator. Figure 3(a) shows the encoded signal that was detected by a high-speed photodiode. The encoded signal was then amplified by an EDFA and sent to the decoder, which had an FBG array similar to that of the encoder, but arranged in a reversed order. After reflection off the second FBG array, the time delays (introduced by the first FBG array) between the chips carried by the different wavelengths were eliminated. Subsequently, the various wavelengths were routed to a 1 mm diameter collimator, and the collimated optical beam was launched toward a 1200 line/mm grating surface that spread the wavelengths along different directions and mapped them onto the active window of the second opto-VLSI processor (decoder), which was loaded with the same phase holograms as those of the first opto-VLSI processor. The coupled-back optical signal was detected by a high-speed photodetector and monitored by using a high-speed digital oscilloscope.

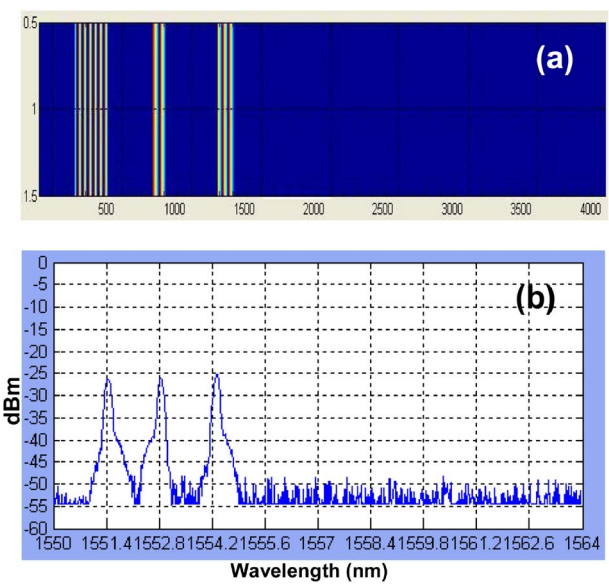

Fig. 2. (Color online) (a) Digital phase holograms loaded on the first and second opto-VLSI processor (encoder) generating a codeword employing λ_1, λ_2, and λ_3. (b) Measured codeword spectrum.

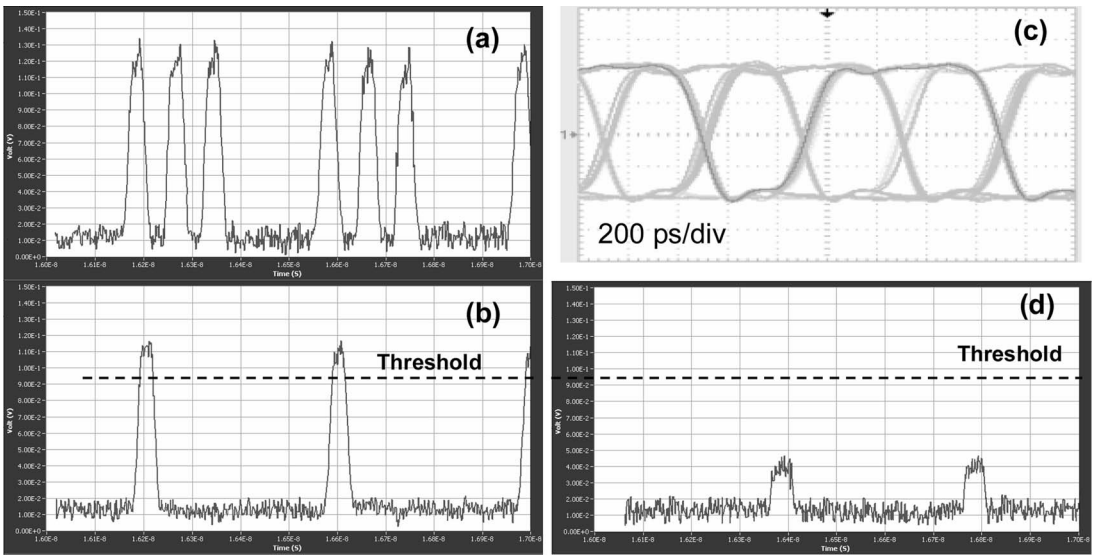

Fig. 3. (a) Encoder output generating a codeword employs λ_1, λ_2, and λ_3. (b) Decoder output when the decoder and encoder codewords were matched. (c) Eye diagram of an error-free transmission. (d) Decoder output when the decoder and encoder codewords were not matched.

When the first and second opto-VLSI processors had the same phase hologram configuration, the original input pulse was recovered, generating a high-peak autocorrelation function as shown in Fig. 3(b). Figure 3(c) shows the eye diagram of an error-free transmission. Note that a mismatch between the encoder and decoder digital phase holograms results in a low-intensity output pulse. To prove this, the digital phase holograms loaded into the pixels blocks of the first opto-VLSI processor (encoder) were left unchanged (i.e., coupling the wavelength components λ_1, λ_2, and λ_3) while the second opto-VLSI processor (decoder) was reconfigured with a codeword assigned to couple back the wavelength components λ_2, λ_4, and λ_5. In this case, a low-amplitude cross-correlation output signal was obtained, as shown in Fig. 3(d). The results shown in Figs. 3(a)–3(d) demonstrate the principle of the proposed wavelengths-encoded OCDMA encoder–decoder structure.

The performance analysis of wavelength-encoded OCDMA systems was recently reported by Rochette *et al.* [2], who showed that multiuser interference (MUI) is the main factor degrading the performance of OCDMA systems. For the proposed OCDMA structure, employing five FBGs allows only ten users to be accommodated when three wavelengths are employed for coding. An additional FBG increases the number of users to 20.

It is important to note that if an FBG array is not employed in the encoder, the opto-VLSI processor alone is able to generate wavelength codewords; however, in this case, all wavelength components occupy a single bit slot, making the OCDMA system susceptible to crosstalk. Therefore, the use of an FBG array is essential in the encoding process to enable the codeword to be spread over many bit slots, thus reducing the interference and improving the security of the encoding.

Finally, it is important to note that with current opto-VLSI fabrication processes, the active window of the opto-VLSI processor can practically be as large as $20\,\mathrm{mm} \times 20\,\mathrm{mm}$, thus enabling up to 32 different wavelengths to be processed simultaneously.

We have proposed and experimentally demonstrated a 2.5 Gbits/s wavelength-encoded OCDMA encoder–decoder structure employing opto-VLSI processors. The attractive feature of the structure is that it enables N encoders at each station to be replaced with a single opto-VLSI processor in conjunction with an FBG array. Codewords have been synthesized at the encoder and at the decoder using computer-generated digital phase holograms, and a high-peak autocorrelation function at the decoder has successfully been observed when the digital phase holograms loaded on the opto-VLSI processors of the decoder and encoder are matched. In "no match" scenarios, low-peak cross-correlation functions have been detected and easily recognized from autocorrelation functions.

References

1. I. Fsaifes, C. Lepers, A.-F. Obaton, and P. Gallion, J. Lightwave Technol. **24**, 3121 (2006).
2. M. Rochette, S. Ayotte, and L. A. Rusch, J. Lightwave Technol. **23**, 1610 (2005).
3. H. Fathallah, L. A. Rusch, and S. LaRochelle, J. Lightwave Technol. **17**, 397 (1999).
4. S. Ayotte, M. Rochette, J. Magne, L. A. Rusch, and S. LaRochelle, J. Lightwave Technol. **23**, 724 (2005).
5. A. Grunnet-Jepsen, A. E. Johnson, E. S. Maniloff, T. W. Mossberg, M. J. Munroe, and J. N. Sweetser, Electron. Lett. **35**, 1096 (1999).
6. Z. Wei, H. M. H. Shalaby, and H. Ghafouri-Shiraz, J. Lightwave Technol. **19**, 1274 (2001).
7. P. Wang and T. Le-Ngoc, J. Lightwave Technol. **23**, 2902 (2005).
8. J. E. McGeehan, S. M. R. Motaghian Nezam, P. Saghari, A. E. Willner, R. Omrani, and P. V. Kumar, J. Lightwave Technol. **23**, 3282 (2005).
9. M. Aljada, K. E. Alameh, and K. Al-Begain, J. Lightwave Technol. **24**, 2779 (2006).